4th Specialty Conference on Coastal, Estuary and Offshore Engineering
4e Conférence spécialisée sur l'ingénierie côtière et en milieu maritime

Montréal, Québec
May 29 to June 1, 2013 / *29 mai au 1 juin 2013*

An accurate finite volume method using fourth order Adams scheme on triangular grids for the Saint-Venant System

A.Beljadid [1] , A.Mohammadian [1] , H.Qiblawey [2]

[1] Department of Civil Engineering, University of Ottawa - E-mail: abelj016@uottawa.ca

[2] Department of Chemical Engineering, Qatar University, P.O. Box 2713, Doha, Qatar

Abstract: In this study, a new finite volume method is developed for shallow water equations on a rotating frame. Most upwind methods, which perform well for gravity waves, lead to large oscillations and/or numerical damping for Rossby waves. We propose an upwind finite volume method on unstructured grids which provides accurate results both for Rossby and gravity waves. This method uses a high-order upwind scheme for the calculation of the numerical flux, and a fourth-order Adams method with an operator splitting approach for temporal integration. The Coriolis term is integrated analytically before and after solving the conservation law. The proposed method can successfully suppress the short-wave numerical noise without damping the long waves. The balance between the flux and Coriolis terms is preserved. This method presents more accurate results than some well-known upwind schemes.

Key word: shallow water, Rossby waves, finite volume method, Adams method

1 Introduction

Many physical phenomena are governed by shallow water equations (SWEs) in the atmosphere, oceans, rivers, etc. In shallow flows, vertical scales are much smaller than horizontal ones, the velocity profile has small changes throughout the depth, and the pressure is assumed to have a hydrostatic profile.

The upwind finite volume method (UFV) schemes use exact or approximate methods to solve the Riemann problem at the interface of computational cells. The most popular scheme which uses the exact solution of the Riemann problem is Godunov's method (1959). Roe's method (1981), which is applied in this work, is the most popular approximate method, but it requires an accurate method to estimate the parameter values near the interface on both sides of the computational cell.

In SWEs with the presence of a source term, some special techniques may be applied for balancing the source and flux terms. Many previous studies had this objective, such as Vazquez-Cendon (1999), Mohammadian et al. (2005, 2006), and Stewart et al. (2011). Other studies have been conducted for large-scale shallow flows to evaluate the performance of the schemes (e.g., Le Roux and Pouliot, 2008; Hanert et al., 2009; Le Roux et al., 2011). A few studies for UFV schemes have been conducted (e.g., Lin et al., 2003; Mohammadian et al., 2008; Beljadid et al., 2012a). Temporal schemes can greatly improve the performance of numerical methods. The most popular temporal scheme is the Total Variation Diminishing (TVD) temporal integration method, developed by Shu and Osher (1988). TVD methods are recommended for their ability to avoid oscillations of the solutions. Beljadid et al. (2012b) studied the performance of UFV schemes using the third-order TVD Runge-Kutta (TVDRK3) method for temporal integration. Several aspects were examined, including mass and energy conservation, numerical diffusion, and numerical oscillations for Kelvin, Yanai, Poincaré, and gravity waves The upwind-centred scheme combined with the TVDRK3 method was found to be a good choice for these types of waves. The results are insensitive to the

values of CFL numbers and present highly accurate results over a wide range of CFL numbers. However, this method fails in the modeling of Rossby waves. These waves have a particular behavior and are difficult to capture by several well-known upwind schemes.
In this paper, a new upwind finite volume method is proposed for linear SWEs on unstructured grids. This method provides accurate results both for Rossby and gravity waves. A high-order spatial scheme based on polynomial fitting is used. Operator splitting and the fourth-order Adams method are used for temporal integration.

The paper is organized as follows: SWEs are presented in Section 2. In Section 3, the proposed finite volume method is described. Section 4 presents some numerical experiments for Rossby and gravity waves using the proposed method for linear SWEs. Finally, concluding remarks complete the study.

2 Shallow water equations

Linear shallow water equations are considered in this work. The 2-D linear SWEs in conservative form are written as:

[1] $$\frac{\partial \mathrm{U}}{\partial t}+\frac{\partial \mathrm{E}}{\partial x}+\frac{\partial \mathrm{G}}{\partial y}=\mathrm{S}$$

and the parameters $\mathrm{U}, \mathrm{E}, \mathrm{G},$ and S are defined by:

[2] $$\mathrm{U}=\begin{bmatrix}\eta\\ u\\ v\end{bmatrix}\quad,\quad \mathrm{E}=\begin{bmatrix}Hu\\ g\eta\\ 0\end{bmatrix}\quad,\quad \mathrm{G}=\begin{bmatrix}Hv\\ 0\\ g\eta\end{bmatrix},\quad \mathrm{S}=\begin{bmatrix}0\\ fv\\ -fu\end{bmatrix}$$

where η represents the water surface elevation, u and v are the depth-averaged velocity components in the x-and y-directions respectively, f is the Coriolis parameter, (H+η) is the total water depth, and g is the gravity acceleration The source term S includes the variable Coriolis parameter ($f=\beta y$), where β is the linear coefficient of variation of f with respect to y .

The linear SWEs can be written in the dimensionless form. The following reference values are used as reference time, length, and velocity scales to convert Equations 1 and 2 into a dimensionless form:

[3] $$T^{*}=\beta^{-1/2}(gH)^{-1/4}\ ,\ L^{*}=\frac{1}{\beta T^{*}}\quad \text{and}\quad U^{*}=V^{*}=\frac{L^{*}}{T^{*}}$$

The resulting system, the Jacobian matrix, and the corresponding eigenvalues and eigenvectors are given in Appendix I.

3 Finite volume method

3.1 Unstructured grid implementation

An upwind finite volume method on an unstructured grid is employed in this paper. The variables are located at the geometric centers of the triangles used as computational grids. The SWEs are integrated over every triangle, which are used as control volumes.

[4] $$\int_{\Omega}\left(\frac{\partial \mathrm{U}}{\partial t}+\frac{\partial \mathrm{E}}{\partial x}+\frac{\partial \mathrm{G}}{\partial y}-\mathrm{S}\right)d\Omega=0$$

where Ω denote the area of the domain.
The previous flux integral is transformed into a boundary integral by using the divergence theorem, as:

[5] $$\int_\Omega \left(\frac{\partial \mathrm{E}}{\partial x} + \frac{\partial \mathrm{G}}{\partial y} \right) d\Omega = \int_\Gamma \mathrm{F} \cdot \mathrm{n} d\Gamma$$

where $\mathrm{F} = \left(\mathrm{E}, \mathrm{G} \right)^t$ is the flux vector, and **n** is the unit outward normal vector to boundary Γ of the domain.

Using equations 4 and 5, we obtain:

[6] $$\frac{d}{dt} \int_\Omega \mathrm{U} dx + \int_\Gamma \mathrm{F} \cdot \mathrm{n} d\Gamma = \int_\Omega \mathrm{S} dx$$

[7] $$\int_\Gamma \mathrm{F} \cdot \mathrm{n} d\Gamma = \sum_{k=1}^{3} \int_{\Gamma_k} \mathrm{F} \cdot \mathrm{n} d\Gamma_k = \sum_{k=1}^{3} \left(\mathrm{F}_k \cdot \mathrm{n}_k \right) l_k$$

where F_k, n_k, Γ_k and l_k, are, respectively, outward flux, the unit outward normal vector, the triangle edges, and the corresponding length. and k is a variable with *k*=1,2,3.

For most schemes, the convective fluxes F_k may be written in the following form:

[8] $\mathrm{F} = 0.5 \left(\mathrm{F}_R + \mathrm{F}_L - \Delta \mathrm{F}^* \right)$ where $\mathrm{F}_L = \mathrm{F}\left(\mathrm{u}_L \right)$ and $\mathrm{F}_R = \mathrm{F}\left(\mathrm{u}_R \right)$ are the left and right flux vectors.

Roe's linearization is used to calculate the flux difference $\Delta \mathrm{F}^*$, which plays the role of stabilization.

[9] $$\Delta \mathrm{F}^* = \sum_{k=1}^{3} \tilde{\alpha}_k \left| \tilde{a}_k \right| \tilde{\mathrm{e}}_k$$

Appendix I gives the details on the projection coefficients $\tilde{\alpha}_k$, the eigenvalues $\tilde{a}_k$, and the eigenvectors $\tilde{\mathrm{e}}_k$ of the approximate Jacobian matrix.

In the κ scheme, U_L, and U_R are calculated at the interface as:

[10]
$$\mathrm{U}_L = \mathrm{U}_w + \frac{s}{4} \left[(1 - ks)(\mathrm{U}_w - \mathrm{U}_{ww}) + \delta (1 + ks)(\mathrm{U}_e - \mathrm{U}_w) \right]$$
$$\mathrm{U}_R = \mathrm{U}_e + \frac{s}{4} \left[(1 - ks)(\mathrm{U}_e - \mathrm{U}_{ee}) + \delta (1 + ks)(\mathrm{U}_w - \mathrm{U}_e) \right]$$

with $\delta = \frac{2L_w}{L_w + L_e}$, where L_w and L_e are defined in Figure 1.

The slope limiter s is calculated using:

[11] $$s = \frac{2\Delta_- \Delta_+}{\Delta_-^2 + \Delta_+^2 + \varepsilon}, \quad \varepsilon > 0$$ with $\Delta_+ = \mathrm{U}_w - \mathrm{U}_{ww}$ and $\Delta_- = \mathrm{U}_e - \mathrm{U}_w$.

Depending on κ, this method leads to the following schemes:

[12] $$\kappa = \begin{cases} 0, & Simplified\ Fromm\ scheme, \\ 1/6, & Cell-based\ third\ order\ upwind, \\ 1/3, & Third-order\ upwind, \\ 1/2, & Quick\ scheme, \\ 1, & Upwind-centered\ scheme \end{cases}$$

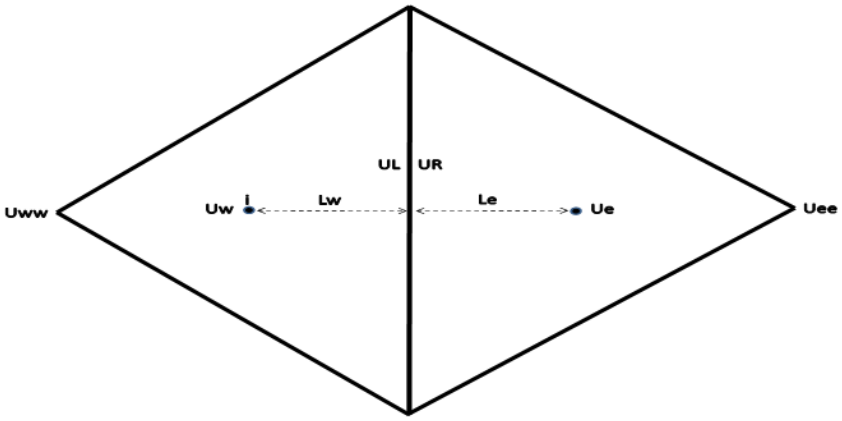

Figure 1: Parameters at the right (R) and left (L) sides of the interface of computational cells

The case $k = -1$ corresponds to the second-order upwind scheme. Based on Beljadid et al. (2012b), since this second-order scheme leads to inaccurate results for Kelvin, Yanai, and Poincaré waves, it is not considered in this paper.

3.2 The proposed high-order upwind scheme

Upwind finite volume methods can be improved if the values of the parameters on both sides of the interface are estimated with more accuracy. In the proposed method we use a high-order upwind interpolation scheme. We use the third-order Lagrange polynomials in $\overline{x}$ and linear interpolation in $\overline{y}$, where the variable $\overline{x}$ denotes the axis perpendicular to the interface and $\overline{y}$ coincides with the interface. The value of U_L is obtained by using interpolation on the basis of three grid points upstream of the interface and one grid point downstream of the interface. The parameter $\mathrm{U}(\overline{x},\overline{y})$ is obtained by the following interpolation:

[13] $$\mathrm{U}(\overline{x},\overline{y}) = \sum_{i=1}^{i=4} L_i^{(l)}(\overline{x})(\mathrm{U}_i - Q^{(l)}(\overline{y}_i)) + Q^{(l)}(\overline{y})$$

where $Q^{(l)}(\overline{y})$ is a polynomial which depends on the variable $\overline{y}$, and $L_i^{(l)}$ is the Lagrange polynomial associated with the cell i, obtained from the parameters of three cells on the left-hand side and one cell on the right-hand side of the interface.

[14] $$L_i^{(l)}(\overline{x}) = \prod_{j=1, j\neq i}^{j=4} \frac{(\overline{x} - \overline{x}_j)}{(\overline{x}_i - \overline{x}_j)}$$

The parameter U_L is obtained by integration along the left-hand side of the interface as:

[15] $\mathrm{U}_L = \frac{1}{l}\int_{\frac{l}{2}}^{\frac{-l}{2}} \mathrm{U}(0^-, \bar{y})d\bar{y}$

where l is the length of the interface of the computational cell.

[16] Since $\sum_{i=1}^{i=4} L_i^{(l)}(\bar{x}) = 1$, thus $\mathrm{U}(\bar{x}, \bar{y}) = \sum_{i=1}^{i=4} L_i^{(l)}(\bar{x})(\mathrm{U}_i - Q^{(l)}(\bar{y}_i) + Q^{(l)}(\bar{y}))$

The form of the above equation allows defining the polynomial $Q^{(l)}$ without a constant. Then, for the linear case, the polynomial $Q^{(l)}$ is defined by $Q(\bar{y}) = \mu\bar{y}$.

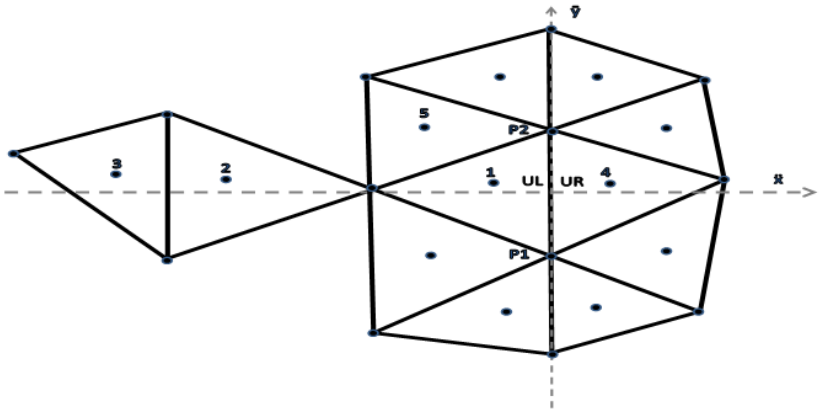

Figure 2: Cells used in the proposed method

In the proposed method, the following first-order expansion is used at the interface extremities:

[17] $\mu = \frac{U_{P_2} - U_{P_1}}{l}$

To estimate the values of U_{P_2} and U_{P_1}, the following linear interpolations are used:

[18] $U_{P_1} = \sum_{i=1}^{i=n} \alpha_i U_{P_{1i}}$ with $\sum_{i=1}^{i=n} \alpha_i = 1$

[19] $dU = \frac{\partial U}{\partial \bar{x}} d\bar{x} + \frac{\partial U}{\partial \bar{y}} d\bar{y}$ then $U_{P_1} = \sum_{i=1}^{i=n} \alpha_i U_{P_{1i}} - (\frac{\partial U}{\partial \bar{x}})_{P_1} \sum_{i=1}^{i=n} \alpha_i \Delta\bar{x}_{1i} - (\frac{\partial U}{\partial \bar{y}})_{P_1} \sum_{i=1}^{i=n} \alpha_i \Delta\bar{y}_{1i}$

where $\Delta\bar{x}_{1i} = \bar{x}_{P_{1i}} - \bar{x}_{P_1}$, $\Delta\bar{y}_{1i} = \bar{y}_{P_{1i}} - \bar{y}_{P_1}$, $(\bar{x}_{P_1}, \bar{y}_{P_1})$ are the coordinates of the point P_1, and $(\bar{x}_{P_{1i}}, \bar{y}_{P_{1i}})$ are the coordinates of the points P_{1i} surrounding the point P_1.

To get an accurate interpolation, we choose α_i for each node by using barycentric coefficients in order to have $\sum_{i=1}^{i=n} \alpha_i \Delta\bar{x}_{1i} = \sum_{i=1}^{i=n} \alpha_i \Delta\bar{y}_{1i} = 0$

3.3 Temporal integration method

In most finite volume models, a Runge-Kutta method is used for temporal integration. In Beljadid et al. (2012b), it was shown that κ schemes combined with the TVD RK3 method led to good results for Kelvin, Yanai, gravity, and inertia gravity waves, and that the upwind-centered scheme is the best one. The κ schemes combined with the TVD RK3 method lead to inaccurate results for Rossby waves.
In this work, the fourth-order Adams method is used as the temporal scheme, with operator splitting for the Coriolis and flux terms. The process includes three stages: in the first and third steps the Coriolis term is integrated analytically, and in the second step the flux term is integrated numerically. In the following, the temporal integration method is explained for linear SWEs. Following Beljadid et. al. (2012a), first, the effect of the source term (the Coriolis effect) is considered:

[20] $$\frac{\partial \mathrm{U}}{\partial t} = \mathrm{S}$$

Then, the flux term is added:

[21] $$\frac{\partial \mathrm{U}}{\partial t} = \mathrm{F} \quad \text{where} \quad \mathrm{F} = -\left(\frac{\partial \mathrm{E}}{\partial x} + \frac{\partial \mathrm{G}}{\partial y} \right)$$

The system with Coriolis term only, i.e.,

[22] $$\frac{\partial u}{\partial t} = fv \ , \quad \frac{\partial v}{\partial t} = -fu \ , \ \frac{\partial \eta}{\partial t} = 0$$

can be solved analytically as:

[23] $$u = u_0 \cos(ft) + v_0 \sin(ft) \ , \ v = v_0 \cos(ft) - u_0 \sin(ft) \ , \ \eta = \eta_0$$

In the following, Δt represents the time-step size and η^n , u^n , and v^n are respectively the water surface elevation and the $x-$ and $y-$velocities at time $t^n = n\Delta t$.

First, equation 20 is integrated over half of the time step:

[24] $$u^* = u^n \cos(f\Delta t/2) + v^n \sin(f\Delta t/2) \ , \ v^* = v^n \cos(f\Delta t/2) - u^n \sin(f\Delta t/2) \ , \ \eta^* = \eta^n$$

Then, equation 21 is integrated over the entire time step:

[25] $$\mathrm{U}^{**} = \mathrm{U}^{*} - \Delta t \sum_{k=1}^{3} \left(\mathrm{F}_k \cdot \mathrm{n}_k \right) l_k$$

and finally, equation 20 is integrated over the second half of the time step, i.e.,

[26] $$u^{\wedge} = u^{**} \cos(f\Delta t/2) + v^{**} \sin(f\Delta t/2) \ , \ v^{\wedge} = v^{**} \cos(f\Delta t/2) - u^{**} \sin(f\Delta t/2) \ , \ \eta^{\wedge} = \eta^{**}$$

The fourth-order Adams method (Appendix I) is used for the temporal integration, as explained below, where the following notation is used:

[27] $$\mathrm{C}^n = \mathrm{U}^{\wedge} - \mathrm{U}^n$$

The fourth-order Adams method uses the fourth-order explicit Adams-Bashforth scheme as the predictor step:

[28] $$\mathrm{U}^{\curlyvee} = \mathrm{U}^{n} + \left(\frac{55}{24}\mathrm{C}^{n} - \frac{59}{24}\mathrm{C}^{n-1} + \frac{37}{24}\mathrm{C}^{n-2} - \frac{9}{24}\mathrm{C}^{n-3} \right)$$

and the fourth-order Adams-Moulton method for the corrector step as:

[29] $$\mathrm{U}^{n+1} = \mathrm{U}^{n} + \left(\frac{9}{24}\mathrm{C}^{\curlyvee} + \frac{19}{24}\mathrm{C}^{n} - \frac{5}{24}\mathrm{C}^{n-1} + \frac{1}{24}\mathrm{C}^{n-2} \right)$$

where $\mathrm{C}^{\curlyvee}$ is the right-hand side of the system calculated using $\mathrm{U}^{\curlyvee}$. In the numerical experiments, we do not need to consider any iteration or modifier at the corrector step. Note that in the above algorithm, the right-hand side of 21, which is the most computationally expensive part, is required to be calculated only twice. The computational cost for the fourth-order Adams method is about half the cost of the fourth-order Runge-Kutta method, in which the right-hand side of 21 must be calculated four times. The fourth-order Adams method uses the values of the parameters and the derivative of the flux function in the earlier steps. Therefore, the first three time steps are required in order to begin the method. In this paper, the first three steps are calculated by using a fourth-order Runge-Kutta method for temporal integration in order to remain consistent in the order of accuracy.

4 Numerical experiments

4.1 Numerical experiments for Rossby waves

Equatorial Rossby waves are found near the equator, hence their name. These waves play an important role in the transfer of energy in the ocean and atmosphere. They propagate westward and are slow (low-frequency) and long. For the equatorial β-plane approximation $f = \beta y$, Rossby waves are exact solutions of linear SWEs, and they are steady state in a moving frame. However, most well-known schemes fail to preserve these solutions. In this section, the analytical solution of SWEs corresponding to the symmetric equatorial Rossby waves of Index 1 is used as the initial condition to test the proposed method. We consider a domain $[0, L]\times[0, L/2]$ with $L = 32$ (non-dimensional) and $X = L/2$. The analytical solution is given as:

[30] $$\begin{cases} v(x,y,t) = -y\cos(kx-\omega t)e^{-y^2/2} \\ r^{+}(x,y,t) = \dfrac{2y^2-1}{k-\omega}\sin(kx-\omega t)e^{-y^2/2} \\ r^{-}(x,y,t) = \dfrac{-1}{k+\omega}\sin(kx-\omega t)e^{-y^2/2} \\ \eta(x,y,t) = \dfrac{r^{-}(x,y,t)-r^{+}(x,y,t)}{2} \\ u(x,y,t) = -\dfrac{r^{-}(x,y,t)+r^{+}(x,y,t)}{2} \end{cases}$$

where $r^{+} = -u-\eta$ and $r^{-} = -u+\eta$ are the Riemann invariants and ω is the root smallest in magnitude of the dispersion relation: $\omega^2 - k^2 - \dfrac{k}{\omega} = 3$

The tests are performed using both the proposed method and the κ schemes, with a fourth-order Adams method as a temporal integration scheme. Figure 3 shows the water surface elevation using the proposed method, the κ schemes, and the analytical solution at time $t = 10T$, where T is the period of the wave. As can be observed in this figure, while the κ schemes have highly damped the waves, the proposed method leads to accurate results for Rossby waves in terms of amplitude and phase errors.

Figure 4 shows the view of the solution in 2-D at time $t = 10T$, and confirms that the solution does not have

any deformation and is preserved in moving frame.

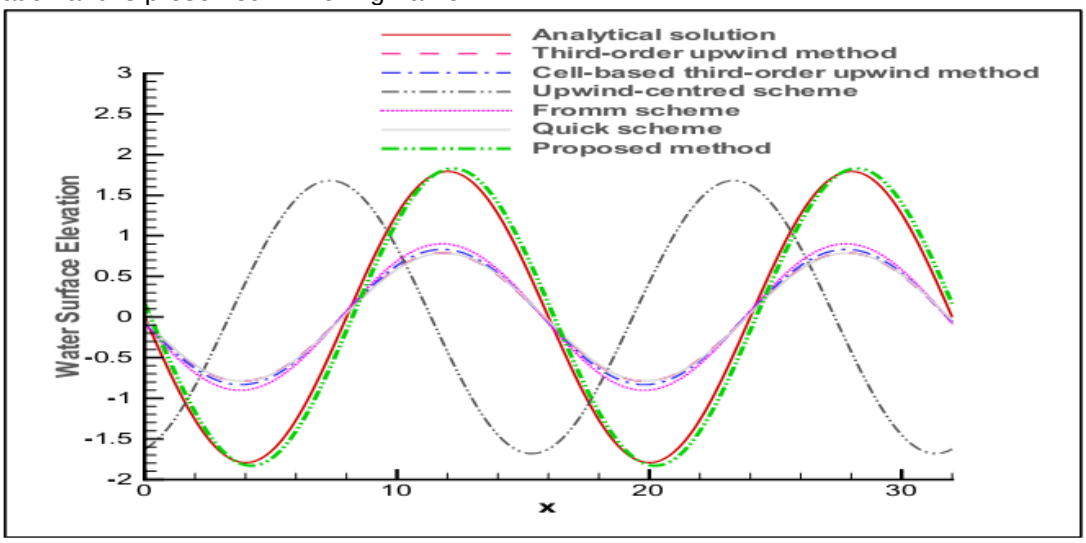

Figure 3: Comparison of numerical solutions using the proposed method, κ schemes, and the analytical solution for Rossby waves at time $t = 10T$ with $CFL = 0.1$ and $cell \quad area = 0.01$

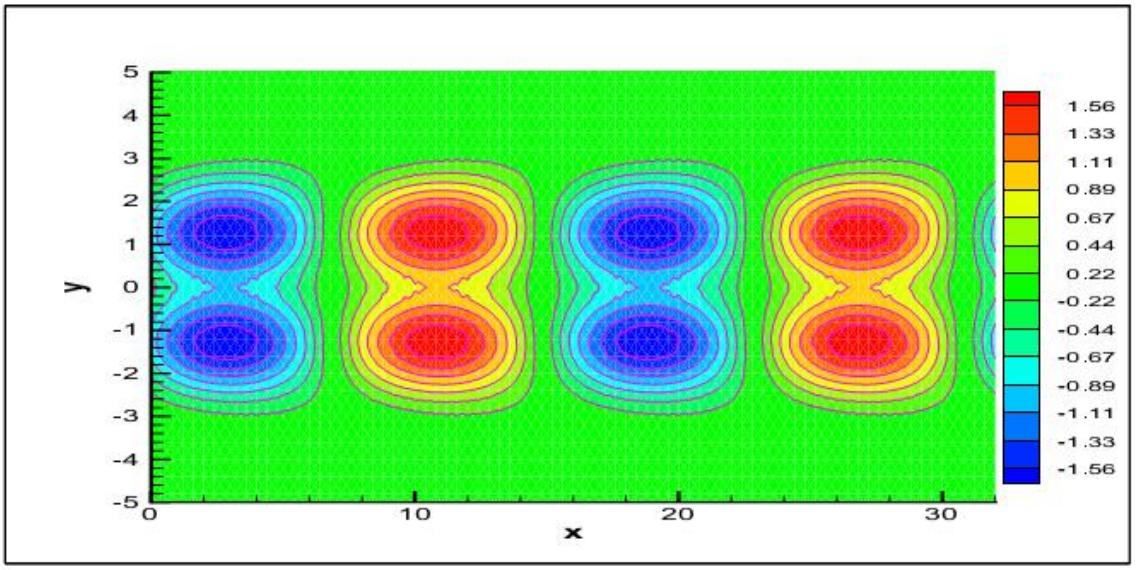

Figure 4: 2-D view of water surface elevation for Rossby waves using the proposed method at time $t = 10T$ with $CFL = 0.1$ and $cell \quad area = 0.01$

4.2 A Gravity Wave Test Case

The following Gaussian distribution of water surface elevation is assumed as the initial condition:

[31] $\eta(x, y, 0) = Ce^{-\delta(x^2+y^2)}$, $u(x, y, 0) = v(x, y, 0) = 0$

We consider the domain $[-150,150]\times[-150,150]$ and the non-dimensional parameter $\delta = 10^{-3}$, as well as $H = 1$ and $C = 0.6$. Figure 5 shows the solutions for the proposed method with $CFL = 0.40$ and cell area $\Omega_m = 2.25$ at time $t = 40$. For the reference solution, the upwind-centred scheme combined with the TVDRK3 method, which is a good choice for the gravity waves, is used with a very fine mesh with cell area $\Omega_m = 1$. The results confirm that the proposed method leads to good results for gravity waves.

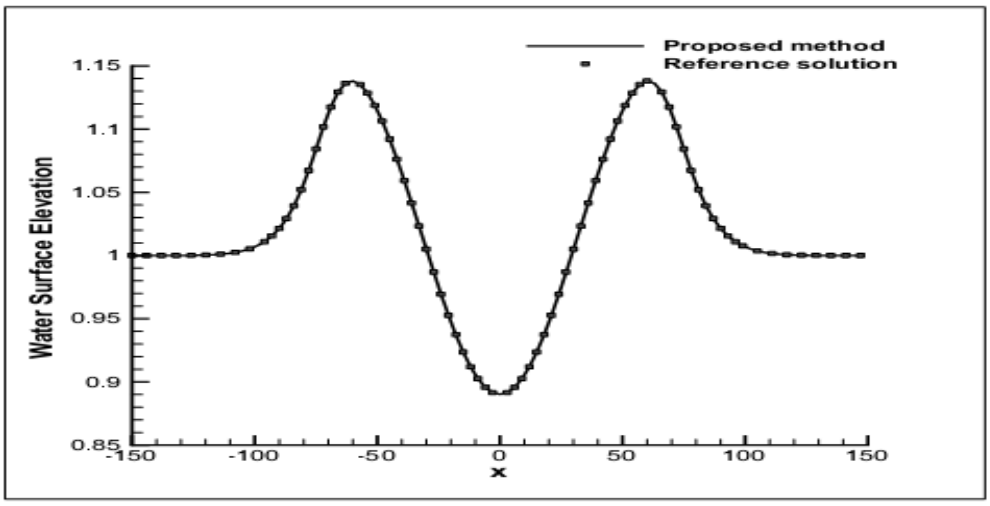

Figure 5: Comparison of the solution using the proposed method and the reference solution at time $t = 40$ with $CFL = 0.40$ and $cell \quad area = 2.25$

CONCLUSION

The proposed method is accurate for linear shallow water equations on unstructured grids for both gravity and Rossby waves. This method uses polynomial fitting with high accuracy for the calculation of the numerical flux. A fourth-order Adams method with an operator splitting approach is used for temporal integration. The proposed method can successfully suppress the short-wave numerical noise without damping the long waves. The numerical experiments confirm that the balance between the flux and Coriolis terms is preserved, which is not the case for the other schemes considered in this paper. Currently we are working on extending this method to non-linear shallow water equations on unstructured grids.

Acknowledgments

This publication was made possible by NPRP grant # 4-935-2-354 from the Qatar National Research Fund (a member of Qatar Foundation). The statements made herein are solely the responsibility of the authors.

References

Beljadid A., Mohammadian A., Qiblawey H., 2012a, Numerical simulation of rotation dominated linear shallow water flows using finite volume methods and fourth order Adams scheme. *Computers & Fluids,* **62**, 64-70.

Beljadid A., Mohammadian A., Le Roux D. Y. , 2012b, Performance of TVD Runge Kutta schemes with upwind finite volume methods over unstructured grids for large scale shallow flows. ***Submitted*** *to International Journal for Numerical Methods in Fluids*.

Godunov S. K., 1959, Finite difference method for numerical computation of discontinuous solutions of the equations of fluid dynamics. *Math. Sbornik,* **47(3)**, 271-306.

Gwo-Fong Lin., Jihn-Sung Lai., Wen-Dar Guo., 2003, Finite-volume component-wise TVD schemes for 2D shallow water equations. *Advances in Water Resources,* **26**, 861-873.

Hanert E., Walters R., Le Roux D. Y., Pietrzak J., 2009, A tale of two elements: P1NC-P1 and RT0. *Ocean Modelling*, **28**, 24-33.

Le Roux D. Y., Dieme M., Sene A., 2011, Time discretization schemes for Poincaré waves in finite-element shallow-water models. *SIAM Journal on Scientific Computing,* **33(5)**, 2217-46

Le Roux D. Y., Pouliot B., 2008, Analysis of numerically-induced oscillations in two-dimensional finite-element shallow water models - part II: free planetary waves. *SIAM Journal on Scientific Computing,* **30**, 1971-91

Mohammadian A., Le Roux D. Y., 2008, Fourier analysis of a class of upwind schemes in shallow water systems for Gravity and Rossby waves. *International Journal for Numerical Methods in Fluids,* **57, 4** , 389-416.

Mohammadian A., Le Roux D. Y., 2006, Simulation of shallow flows over variable topography using

unstructured grid. *International Journal for Numerical Methods in Fluids,* **48(10)**, 1149-74
Mohammadian A., Le Roux D. Y., Tajrishi M., Mazaheri K., 2005, A Mass Conservative Scheme for Simulating Shallow Flows over Variable Topography Using Unstructured Grid. *Advances in Water Resources,* **Vol. 28**, pp. 523-537.
Roe P. L., 1981, Approximate Riemann solvers, parameter vectors, and difference schemes. *Journal of Computational Physics,* **43**,357-372
Stewart A.L, Dellara P.J., Johnson E., 2011, Numerical simulation of wave propagation along a discontinuity in depth in a rotating annulus. *Computers & Fluids,* **46(1)**, 442-7.
Vazquez-Cendon M.E., 1999, Improved treatment of source terms in upwind schemes for the shallow water equations in channels with irregular geometry. *Journal of Computational Physics,* **148**, 497-526.

Appendix I: The Jacobian matrix for SWEs

I.1 The Jacobian matrix for linear equations

The matrix $\tilde{\mathrm{J}}$ satisfies $\Delta \mathrm{F} = \tilde{\mathrm{J}}\,\Delta \mathrm{u}$ with

[32] $$\tilde{\mathrm{J}} = \frac{\partial(\mathrm{F}\cdot \mathrm{n})}{\partial \mathrm{u}} = \begin{pmatrix} 0 & Hn_x & Hn_y \\ gn_x & 0 & 0 \\ gn_y & 0 & 0 \end{pmatrix} \quad \text{where } c = \sqrt{gH}\,.$$

The eigenvalues of $\tilde{\mathrm{J}}$ are given by $\tilde{a}_1 = c,\ \tilde{a}_2 = 0,\ \tilde{a}_3 = -c,$ with the corresponding eigenvectors

[33] $$\tilde{\mathrm{e}}_1 = \begin{pmatrix} 1 \\ \lambda_0 n_x \\ \lambda_0 n_y \end{pmatrix},\ \tilde{\mathrm{e}}_2 = \begin{pmatrix} 0 \\ -\lambda_0 n_y \\ \lambda_0 n_x \end{pmatrix},\ \tilde{\mathrm{e}}_3 = \begin{pmatrix} 1 \\ -\lambda_0 n_x \\ -\lambda_0 n_y \end{pmatrix} \quad \text{where} \quad \lambda_0 = \sqrt{\frac{g}{H}}$$

The coefficients $\tilde{\alpha}_k$, *k*=1,2,3, are computed as

[34] $$\tilde{\alpha}_1 = \frac{\Delta h}{2} + \frac{1}{2\lambda_0}\left[\Delta u\, n_x + \Delta v\, n_y\right],\ \tilde{\alpha}_2 = \frac{1}{\lambda_0}\left[\Delta v\, n_x - \Delta u\, n_y\right],\ \tilde{\alpha}_3 = \frac{\Delta h}{2} - \frac{1}{2\lambda_0}\left[\Delta u\, n_x + \Delta v\, n_y\right]$$

The eigenvalues and eigenvectors of the nondimensional system can be calculated using those of the original system, by simply setting $H = g = 1.$

I.2 The fourth-order adams method

For an ODE defined by

[35] $$\frac{dU}{dt} = f(U,t)$$

The fourth-order Adams method uses the fourth-order Adams-Bashforth scheme as predictor

[36] $$U^{\curlyvee} = U^n + \Delta t\left(\frac{55}{24} f^n - \frac{59}{24} f^{n-1} + \frac{37}{24} f^{n-2} - \frac{9}{24} f^{n-3}\right)$$

and the fourth-order Adams-Moulton scheme as corrector

[37] $$U^{n+1} = U^n + \Delta t\left(\frac{9}{24} f^{\curlyvee} + \frac{19}{24} f^n - \frac{5}{24} f^{n-1} + \frac{1}{24} f^{n-2}\right) \quad \text{where} \quad f^n = f(U^n, n\Delta t)$$